

# Validation of OMI tropospheric NO<sub>2</sub> column data using MAX-DOAS measurements deep inside the North China Plain in June 2006

H. Irie<sup>1</sup>, Y. Kanaya<sup>1</sup>, H. Akimoto<sup>1</sup>, H. Tanimoto<sup>2</sup>, Z. Wang<sup>3</sup>, J.F. Gleason<sup>4</sup>, and E.J. Bucsela<sup>5</sup>

<sup>1</sup>Frontier Research Center for Global Change, Japan Agency for Marine-Earth Science and Technology, 3173-25 Showa-machi, Kanazawa-ku, Yokohama, Kanagawa 236-0001, Japan

<sup>2</sup>National Inst. for Environmental Studies, 16-2, Onogawa, Tsukuba, Ibaraki 305-8506, Japan

<sup>3</sup>LAPC/NZC, Institute of Atmospheric Physics, Chinese Academy of Sciences, Beijing, 100029, China

<sup>4</sup>Atmospheric Chemistry and Dynamics branch, NASA Goddard Space Flight Center, Greenbelt, MD 20771-0000, USA

<sup>5</sup>SRI International, Menlo Park, CA 94107, USA

Received: 4 March 2008 – Accepted: 1 April 2008 – Published: 25 April 2008

Correspondence to: H. Irie (irie@jamstec.go.jp)

Published by Copernicus Publications on behalf of the European Geosciences Union.

8243

## Abstract

A challenge for the quantitative analysis of tropospheric nitrogen dioxide (NO<sub>2</sub>) column data from satellite observations is posed mainly by the lack of satellite-independent observations for validation. We performed such observations of the tropospheric NO<sub>2</sub> column using the ground-based Multi-Axis Differential Optical Absorption Spectroscopy (MAX-DOAS) technique in the North China Plain (NCP) from 29 May to 29 June 2006. Comparisons between tropospheric NO<sub>2</sub> columns measured by MAX-DOAS and the Ozone Monitoring Instrument (OMI) onboard the Aura satellite indicate that OMI data (the standard product, version 3) over NCP may have a positive bias of  $1.6 \times 10^{15}$  molecules cm<sup>-2</sup> (20%), where the estimated random error in the OMI data is  $0.6 \times 10^{15}$  molecules cm<sup>-2</sup> or approximately 8%. Combining these results with literature validation results for the US, Europe, and Pacific Ocean suggests that a bias of +20%/–30% is a reasonable estimate, accounting for different regions. Considering the uncertainty estimated here will pave the way for quantitative studies using OMI NO<sub>2</sub> data, especially over NCP.

## 1 Introduction

Since 1995, satellite observations have provided tropospheric column data for nitrogen dioxide (NO<sub>2</sub>) on a global scale (e.g., Richter et al., 2005). The satellite observations have been shown to be crucial, for instance, to the estimation of recent trends in tropospheric NO<sub>2</sub> over several important regions, including the North China Plain (NCP) of the People's Republic of China (Richter et al., 2005; Irie et al., 2005; van der A et al., 2006), and to the systematic evaluation of global atmospheric chemistry models (van Noije et al., 2006). However, although a quantitative basis for analyzing satellite data should be provided by comparisons with other independent measurements, such satellite-independent measurements are very limited. Some satellite-independent measurements were made over the US, Europe, and Pacific Ocean (Brinksma et al.,

8244

2008<sup>1</sup>; Bucsela et al., 2008<sup>2</sup>; Celarier et al., 2008<sup>3</sup>), but none over NCP (Irie et al., 2005). In addition, tropospheric data can be obtained by a single satellite-borne instrument with a frequency of no more than once per day for one location at midlatitudes, because of the satellite orbit and interference by clouds. Furthermore, it is generally  
5 very difficult to derive vertical profile information in the troposphere from satellite observations.

To overcome these shortcomings in satellite observations of the tropospheric NO<sub>2</sub>, we performed ground-based Multi-Axis Differential Optical Absorption Spectroscopy (MAX-DOAS) measurements at two sites at the base and summit of Mt. Tai in NCP  
10 between 29 May and 29 June, 2006. The base site is referred to as “Tai’an” (36.2° N, 117.1° E, 126 m a.s.l.) and the mountaintop site located only 10 km north of Tai’an is referred to as “Mt. Tai” (36.3° N, 117.1° E, 1534 m a.s.l.). The measurements were made as a part of our intensive field measurement campaign. The retrieval of the tropospheric NO<sub>2</sub> column is performed using the vertical profiles of the box-air-mass-factor ( $A_{\text{box}}$ ), which is defined as the air mass factor for a given layer (Wagner et al.,  
15

<sup>1</sup>Brinksma, E. J., Pinardi, G., Braak, R., Volten, H., Richter, A., Schönhardt, A., van Roozendaal, M., Fayt, C., Hermans, C., Dirksen, R.J., Vlemmix, T., Berkhout, A. J. C., Swart, D. P. J., Oetjen, H., Wittrock, F., Wagner, T., Ibrahim, O. W., de Leeuw, G., Moerman, M., Curier, R.L., Celarier, E. A., Knap, W. H., Veefkind, J. P., Eskes, H. J., Allaart, M., Rothe, R., Peters, A. J. M., and Levelt, P. F.: The 2005 and 2006 DANDELIONS NO<sub>2</sub> and aerosol validation campaigns, submitted to J. Geophys. Res., 2008.

<sup>2</sup>Bucsela, E. J., Perring, A. E., Cohen, R. C., Boersma, K. F., Celarier, E. A., Cleason, J. F., Wenig, M. O., Bertram, T. H., Wooldridge, P. J., Dirksen, R., and Veefkind, J. P., Comparison of NO<sub>2</sub> in situ aircraft measurements with data from the Ozone Monitoring Instrument, submitted to J. Geophys. Res., 2008.

<sup>3</sup>Celarier, E. A., Brinksma, E. J., Gleason, J. F., Veefkind, J. P., Cede, A., Herman, J. R., Ionov, D., Goutail, F., Pommeraeu, J.-P., Lambert, J.-C., van Roosendaal, M., Pinardi, G., Bojkov, B., Mount, G., Spinei, E., Sander, S. P., Bucsela, E. J., Swart, D. P. J., Volten, H., Kroon, M., and Levelt, P. F.: Overview of the validation of nitrogen dioxide retrieved from the Ozone Monitoring Instrument, submitted to J. Geophys. Res., 2008.

8245

2007). The  $A_{\text{box}}$  profile is determined from the MAX-DOAS itself, as the analysis of absorption by the oxygen collision complex (O<sub>2</sub>-O<sub>2</sub>, or O<sub>4</sub>) gives a vertical profile of the aerosol extinction coefficient (AEC) that controls the effective path of sunlight reaching the MAX-DOAS system (Irie et al., 2008). In the present study, we first assess the  
5 MAX-DOAS measurements by two approaches: (1) using the aerosol optical depth (AOD) data from the Moderate Resolution Imaging Spectrometer (MODIS) to verify the determined  $A_{\text{box}}$  profiles and (2) using the NO<sub>2</sub> volume mixing ratio (VMR) data obtained in situ by a chemiluminescence technique at the top of Mt. Tai to confirm the NO<sub>2</sub> retrieval. On the basis of these assessments, the standard product (SP) of tropospheric NO<sub>2</sub> column data (version 3) obtained by the Ozone Monitoring Instrument (OMI) (Levelt et al., 2006) onboard NASA’s Earth Observing System (EOS) Aura satellite over NCP is validated for the first time, through comparisons with MAX-DOAS data.  
10 The OMI data are characterized also from the viewpoint of the diurnal variation pattern of the tropospheric NO<sub>2</sub> column based on its measurements by MAX-DOAS.

## 15 **2 Measurements**

### 2.1 MAX-DOAS

From 29 May to 29 June, 2006, we performed MAX-DOAS measurements at two sites, Tai’an and Mt. Tai, in NCP. At Tai’an, we operated a MAX-DOAS instrument employing a miniaturized ultraviolet/visible (UV/VIS) spectrometer (B&W TEK Inc., BTC111),  
20 a single telescope, and a movable mirror, to conduct sequential measurements of scattered sunlight at five different elevation angles (ELs) of 5°, 10°, 20°, 30°, and 90° every 30 min. The line of sight (LOS) for off-axis geometries was directed northward. On the other hand, the MAX-DOAS system operated at Mt. Tai employed a two-dimensional CCD (charge-coupled device) array detector (Andor Technology, DV-420A-OE; 1024×256 pixels) and five telescopes, which were all directed south but with  
25 different ELs fixed at -5°, 5°, 10°, 20°, and 30°. To acquire a reference spectrum with

8246

the same instrument line shape as that of the off-axis measurements, a mirror was periodically inserted into the field of view (FOV) of each telescope, directing the viewing path to the zenith sky (EL=90°). A 6-min zenith-sky measurement was made every 30 min. The five different measured spectra were projected onto the CCD detector simultaneously, with a 30-pixel track for each spectrum. Both MAX-DOAS systems placed at Tai'an and Mt. Tai were operated throughout the day. More information on these MAX-DOAS instruments can be found elsewhere (Irie et al., 2008; Inomata et al., 2008).

For respective measurements at Tai'an and Mt. Tai, we used a common retrieval algorithm, described below. To the fitting window of 460–490 nm we applied the DOAS spectral fitting algorithm identical to that described by Irie et al. (2008). The retrieval algorithm takes into account absorption by trace gases NO<sub>2</sub>, O<sub>4</sub>, O<sub>3</sub>, and H<sub>2</sub>O, and the Ring and undersampling effects. The quantity retrieved with this DOAS method is the so-called differential slant column density ( $\Delta$ SCD), which is defined as the difference between the column concentration integrated along the sunlight path measured at a low EL (EL<90°) and that at EL=90°. The O<sub>4</sub> $\Delta$ SCD values were next converted using our aerosol retrieval algorithm (Irie et al., 2008) to the AOD and the vertical profile of the AEC at a wavelength of 476 nm, which corresponds to the O<sub>4</sub> cross section-weighted mean wavelength over 460–490 nm. The aerosol retrieval was made using the optimal estimation method (Rodgers, 2000; Irie et al., 2008) and a three-dimensional Monte Carlo radiative transfer model, MCARaTS (Iwabuchi, 2006). MCARaTS is a parallelized three-dimensional radiative transfer model utilizing the forward-propagating Monte Carlo photon transport algorithm. For a given layer, the  $A_{\text{box}}$ , which characterizes the ratio of partial slant to vertical columns, was calculated as an intensity-weighted average path length. The  $A_{\text{box}}$  calculations by MCARaTS have been validated through comparisons with other radiative transfer models (Wagner et al., 2007). A lookup table (LUT) of  $A_{\text{box}}$  vertical profile for different sets of aerosol profiles and observation geometries was created and used to find the optimal aerosol and  $A_{\text{box}}$  profiles that account for O<sub>4</sub> $\Delta$ SCD values measured at all ELs. The radiative transfer

8247

model calculations made in the present study assume a single scattering albedo of 0.90, an asymmetry parameter of 0.65, and a surface albedo of 0.10. The overall intrinsic uncertainty in the retrieved AOD, including an impact of these assumptions, was estimated generally to be 30% (Irie et al., 2008). It should be noted, however, that the MAX-DOAS AOD can be underestimated when optically thick aerosols are present at high altitudes (Irie et al., 2008). While MAX-DOAS measurements are very insensitive to high-altitude clouds (above ~2 km), it is likely that the retrieved AOD includes a 30%-reduced contribution of cloud optical depth at lower altitudes (Irie et al., 2008). These effects, however, do not essentially impact the OMI validation results, as discussed later.

Since the  $A_{\text{box}}$  profile is a function of aerosol profile in the LUT, the  $A_{\text{box}}$  is also uniquely determined by the aerosol retrieval method. Using the  $A_{\text{box}}$  profiles and a nonlinear iterative inversion method very similar to that of the aerosol retrieval, we converted the NO<sub>2</sub> $\Delta$ SCD values to the tropospheric vertical column density (VCD) and the vertical profile of NO<sub>2</sub>. By fitting the NO<sub>2</sub> $\Delta$ SCD values, we retrieved the NO<sub>2</sub> vertical profile represented by four parameters: VCD,  $f_1$ ,  $f_2$ , and  $f_3$ . The  $f$  values are the profile shape-determining parameters, each of which ranges between 0 and 1, as defined similarly by Irie et al. (2008) for the aerosol retrieval. Partial VCD values for 0–1, 1–2, and 2–3 km are then given by VCD  $f_1$ , VCD(1- $f_1$ ) $f_2$ , and VCD (1- $f_1$ ) (1- $f_2$ ) $f_3$ , respectively, and the partial VCD at 3–15 km is given by VCD (1- $f_1$ ) (1- $f_2$ ) (1- $f_3$ ). Assuming a profile shape within each layer (e.g., an exponential profile shape within the 0–1 km layer), a continuous NO<sub>2</sub> profile from the surface to 15 km was constructed. An assumption of the stratospheric NO<sub>2</sub> above 15 km was made based on a climatological dataset from Halogen Occultation Experiment (HALOE) measurements at midlatitudes.

Note that the units of the resulting partial VCD values, such as VCD  $f_1$  for the 0–1-km layer, gives number concentration (VCD  $f_1 \Delta z$ , where  $\Delta z=1$  km). This was converted to VMR using US standard atmosphere temperature and pressure data, which were scaled to match the surface values recorded at the location and time of the measurements.

8248

An accurate error estimate is a major challenge for remote sensing measurements, including MAX-DOAS. For each retrieval, we estimated the random error from the retrieval covariance matrix. In this estimate, we used the measurement error covariance matrix constructed from the residual that arose in fitting the  $\text{NO}_2\Delta\text{SCD}$  values. This is because the residual was much larger than the  $\text{NO}_2\Delta\text{SCD}$  error quantified from the DOAS fitting residuals. The systematic error was estimated as the change on the retrieved value that was found when we varied the AOD by an additional  $\pm 30\%$ . For all the measurements at Tai'an and Mt. Tai, the mean values of the random and systematic errors estimated in this way are summarized in Tables 1 and 2, respectively. In Tables 1 and 2, the mean values of the maximum  $A_{\text{box}}$  at different ELs for each retrieval ( $A_{\text{box,max}}$ ) and the mean horizontal distances ( $D$ ), over which the measured sunlight traversed, are also shown for each layer. The  $D$  values were calculated as  $\sqrt{A_{\text{box,max}}^2 - 1}$ , and both the  $A_{\text{box,max}}$  and  $D$  values provide a measure of the MAX-DOAS measurement sensitivity. Consistent with previous work showing that the highest sensitivity of MAX-DOAS measurements occurs in the layer nearest the instrument (Hönninger et al., 2004; Frieß et al., 2006; Irie et al., 2008), the  $A_{\text{box,max}}$  and  $D$  values at 0–1 km are larger than at 1–2 km for MAX-DOAS measurements at Tai'an. For the measurement geometry at Mt. Tai, the  $A_{\text{box,max}}$  and  $D$  values for the 0–1-km layer are as small as 1.2 and 0.7 km, respectively, indicating that the measured sunlight could not penetrate deep inside the layer. Therefore, we analyze only the VMR data at 1–2 km below, for measurements at Mt. Tai.

## 2.2 In situ $\text{NO}/\text{NO}_x/\text{NO}_y$ instrument

At the top of Mt. Tai, the  $\text{NO}_2$  VMR was measured by a custom-built  $\text{NO}/\text{NO}_x/\text{NO}_y$  instrument based on a chemiluminescence  $\text{NO}$  analyzer coupled with converters for  $\text{NO}_2$  and total reactive nitrogen oxides ( $\text{NO}_y$ ).  $\text{NO}$  was measured using a high-sensitivity chemiluminescence analyzer (Thermo Environmental Instruments Inc., 42CTL).  $\text{NO}_2$  was detected as  $\text{NO}$  following narrow-band photo-dissociation by a light-emitting diode

8249

(LED) between 390 and 405 nm (Droplet Measurement Technologies, BLC). The use of an LED-based converter is suitable for a field operation, especially at a mountainous site, because it has a longer lifetime, emits less heat, and consumes less energy than a conventional lamp does. The conversion efficiency of  $\text{NO}_2$  was typically 50% at a flow rate of  $\sim 1$  s.l.p.m.  $\text{NO}_y$  was catalytically converted to  $\text{NO}$  on a molybdenum surface heated at  $320^\circ\text{C}$ . Two solenoid valves placed between the converters and the chemiluminescence detector provided sequential detection of  $\text{NO}$ ,  $\text{NO}_x$ , and  $\text{NO}_y$ . The time resolution was 3 min for each mode. The  $\text{O}_3$  used for  $\text{NO}-\text{O}_3$  chemiluminescence was generated by a silent discharge of dust-filtered air taken from ambient air. Sensitivity and background levels of  $\text{NO}$ ,  $\text{NO}_x$ , and  $\text{NO}_y$  were investigated in detail by the gas-phase titration (GPT) technique. National Institute for Environmental Studies (NIES) gas standards used were gravimetrically prepared at 2 ppmv and intercompared to National Oceanic and Atmospheric Administration (NOAA) standards. Agreement between NIES and NOAA standards was within 0.5%. For a 1-min integration the detection limit for  $\text{NO}$  was estimated to be  $\sim 100$  pptv, and for  $\text{NO}_2$  it was  $\sim 200$  pptv. The instrument was computer-controlled for switching flow valves, lamp, sample and  $\text{O}_2$  flows, and data acquisition.

## 2.3 OMI

The OMI instrument is a nadir-viewing imaging spectrometer measuring direct and atmosphere-backscattered sunlight in the UV/VIS range from 270 to 500 nm (Levelt et al., 2006). It was launched onboard the Aura satellite on 15 July 2004, and put into a Sun-synchronous, polar orbit at an altitude of about 705 km with an equator crossing time between 13:40 and 13:50 LT. OMI employs two two-dimensional CCD detectors that record the (ir)radiance spectrum in UV (270–310 nm and 310–365 nm) and VIS (365–500 nm) regions, respectively. Over the OMI FOV ( $114^\circ$ ), 60 discrete viewing angles are distributed perpendicular to the flight direction. The FOV corresponds to a 2600-km-wide spatial swath on the Earth's surface, achieving daily global measurements. Nadir spatial resolution ranges from  $13\times 24$  to  $24\times 48$   $\text{km}^2$ , depending on the

8250

operation mode.

The present study uses the SP dataset (version 3) of OMI tropospheric NO<sub>2</sub> columns retrieved based on the methods described by Bucsele et al. (2006) and Celarier et al. (2008<sup>3</sup>). We used the data referred to as the “ColumnAmountNO2Trop” in data files obtained from the NASA Goddard Earth Sciences Data and Information Services Center (GES-DISC). Another OMI SP data product, “ColumnAmountNO2TropPolluted”, was almost equivalent to the “ColumnAmountNO2Trop” data for the dataset analyzed here, as the differences between the two values were very small ( $<0.2 \times 10^{15}$  molecules cm<sup>-2</sup>). The “below cloud” NO<sub>2</sub> column has been added for more realistic tropospheric column estimates, but only data with the cloud fraction less than 0.1 are analyzed below. The monthly average map of the OMI tropospheric NO<sub>2</sub> columns for June 2006 is shown in Fig. 1. Pronounced high tropospheric NO<sub>2</sub> columns exceeding  $10 \times 10^{15}$  molecules cm<sup>-2</sup> were extensively distributed over the NCP region, including MAX-DOAS measurement sites at/near Mt. Tai. In particular, considerable amounts of tropospheric NO<sub>2</sub> exceeding  $20 \times 10^{15}$  molecules cm<sup>-2</sup> were observed around Beijing, Tanshan (east of Beijing), a mountain/NCP-edge area including Shijiazhuang, Xingtai, and Handan (southwest of Beijing), Jinan (north of Mt. Tai), and Shanghai.

### 3 Results and Discussion

#### 3.1 Assessment of MAX-DOAS data

In this section, we describe the assessment of both the aerosol and NO<sub>2</sub> measurements made with the MAX-DOAS instrument. First, we use the MODIS AOD data (collection 5) to assess the MAX-DOAS aerosol retrievals that determine the  $A_{\text{box}}$  vertical profiles. Monthly mean AOD values at 550 nm measured by MODIS instruments for June 2006 are shown in Fig. 2. Two datasets from MODIS/Terra and MODIS/Aqua have been unified. Similar to the tropospheric NO<sub>2</sub> map shown in Fig. 1, high AOD values occurred over large areas of the NCP. Peak AOD values are found in the south-

8251

eastern part of NCP, presumably due to crop residue burning associated with the local harvest of winter wheat in this season, as discussed by Fu et al. (2007) using satellite formaldehyde (from GOME) and hot spot data (from ATSR) and the GEOS-CHEM global chemical transport model.

In Fig. 3a, a time series of AOD values at 476 nm derived from the MAX-DOAS at Tai'an is compared with that of mean MODIS AOD data obtained within 0.1° latitude and longitude of Tai'an. Note that the plotted MODIS AOD values have been converted from the original AOD values at 470 nm using MODIS Ångström exponent data. The MODIS data with a cloud fraction less than 0.1 were used. Good agreement between MAX-DOAS and MODIS AOD values is seen, especially with respect to the pattern of temporal variation. This agreement is surprising under such considerably high-AOD conditions, where MAX-DOAS measurements show that the mean AEC value for the lowest 1-km layer was as high as  $0.7 \text{ km}^{-1}$  on average over the measurement period (Fig. 3b). The mean AEC value corresponds to a visibility of only 5.6 km, based on the Koschmieder equation (Jacobson, 1999).

Although the MAX-DOAS and MODIS measurements were both made under such severe conditions, positive correlations were obtained at MODIS AOD  $<1.2$  (Fig. 4). For most cases with MODIS AOD  $<1.6$ , agreement is within 30%. However, significant deviations occur at MODIS AOD  $>1.2$  for both comparisons with MODIS/Terra and MODIS/Aqua. Such large deviations are not expected to be due to an error in the MODIS data, because the comprehensive comparisons have shown better agreement with AERONET (Aerosol Robotic Network) measurements (Remer et al., 2005), suggesting an underestimate in MAX-DOAS AOD values. A similar tendency for occasional underestimation has been discussed in our previous work, where we have attributed it to the presence of optically thick aerosols at high altitudes and/or clouds in the lower troposphere (Irie et al., 2008).

As mentioned above, MODIS AOD data with a cloud fraction less than 0.1 have been compared to the MAX-DOAS AOD data in Figs. 3 and 4. In addition, for the analyzed  $0.1^\circ \times 0.1^\circ$  grid centered on Tai'an, standard deviations that may reflect spatial

8252

inhomogeneity of the optical depth due to aerosols (and potentially clouds) do not show distinct differences in spatial inhomogeneity between cases of MODIS AODs less and greater than 1.2, suggesting that most of the comparisons have been made under cloud-free conditions. Therefore, it is most likely that the significant deviations  
5 seen at MODIS AOD >1.2 were caused by the presence of high-altitude optically thick aerosols (above ~2 km), to which the sensitivity of MAX-DOAS measurements was too low. However, the 30%-change in MAX-DOAS AOD influences the retrieved NO<sub>2</sub> VCD and VMR by only about 10% (Table 1), indicating that an underestimate in MAX-DOAS AOD is a minor problem for the NO<sub>2</sub> retrievals. This is confirmed below by making  
10 additional comparisons with in situ NO<sub>2</sub> measurements performed at the summit of Mt. Tai.

Figure 5a shows two sets of MAX-DOAS NO<sub>2</sub> VMR data from Tai'an and Mt. Tai, which are compared with in situ NO<sub>2</sub> VMR data. The data plotted are the mean NO<sub>2</sub> VMRs at 1–2 km above the surface (1626±500 m a.s.l.) for MAX-DOAS measurements  
15 and the NO<sub>2</sub> VMRs at the mountaintop (1534 m a.s.l.) for the in situ measurements. Thus, air masses measured by these MAX-DOAS and in situ instruments differed, especially in terms of the representative altitude and air mass volume. These differences made it difficult to assess the MAX-DOAS data using a correlation analysis. We find, however, that on average these different datasets show very similar values  
20 (Fig. 5a). The mean differences of NO<sub>2</sub> VMRs measured by MAX-DOAS instruments at Tai'an and Mt. Tai from in situ NO<sub>2</sub> data were as small as  $-0.01 \pm 0.60$  ppbv and  $-0.29 \pm 0.65$  ppbv, respectively. These agreements provide confidence in our MAX-DOAS retrieval methods and hence the accuracy of MAX-DOAS NO<sub>2</sub> VMRs at 0–1 km, shown in Fig. 5b, because the sensitivity of MAX-DOAS measurements at Tai'an to the  
25 layer of 0–1 km should be much higher than that to the 1–2-km layer (Table 1), as discussed earlier. This further ensures the accuracy of the MAX-DOAS tropospheric NO<sub>2</sub> column data, because in general most NO<sub>2</sub> should be at altitudes below 2 km and our MAX-DOAS retrieval algorithm takes into account the profile above 2 km as well.

8253

### 3.2 Diurnal variation of tropospheric NO<sub>2</sub>

For the period from 29 May to 29 June 2006, the time series plot of the tropospheric NO<sub>2</sub> VCDs derived from MAX-DOAS measurements at Tai'an is shown in Fig. 6. The median tropospheric VCD for the period was  $9.4 \times 10^{15}$  molecules cm<sup>-2</sup>, where central  
5 67% of the data were widely distributed between  $6.1 \times 10^{15}$  and  $15.7 \times 10^{15}$  molecules cm<sup>-2</sup>. The large temporal variation of NO<sub>2</sub> observed here was caused predominantly by its diurnal variation, not day-to-day variation, as seen in Fig. 6. To quantify the diurnal variation, the hourly median tropospheric NO<sub>2</sub> VCDs measured by MAX-DOAS are plotted against the local time of the measurements (Chinese standard time, CST)  
10 in Fig. 7a. The daily mean values of OMI NO<sub>2</sub> VCDs obtained at locations within 0.1° latitude and longitude of Tai'an are also plotted to characterize the OMI data from the viewpoint of the diurnal variation pattern.

As seen in Fig. 7, MAX-DOAS measurements provided the complete diurnal variations of the NO<sub>2</sub> tropospheric VCD and VMR at 0–1 km in daytime. The tropospheric  
15 NO<sub>2</sub> VCD (VMR at 0–1 km) was highest at  $\sim 15 \times 10^{15}$  molecules cm<sup>-2</sup> ( $\sim 5$  ppbv) in the early morning (06:00–09:00 CST) and dropped to  $\sim 7 \times 10^{15}$  molecules cm<sup>-2</sup> ( $\sim 2$  ppbv) at 13:00–15:00 CST. This indicates that the OMI measurements were made when the tropospheric NO<sub>2</sub> VCD was lowest in its typical diurnal cycle.

Interestingly, the diurnal variation pattern in the tropospheric NO<sub>2</sub> VCD measured by  
20 MAX-DOAS indicates that the ratio of the tropospheric VCDs at 10:00 and 13:30 LTs was greater than unity, consistent with that derived from two different types of satellite measurements (by SCIAMACHY around 10:00 LT and OMI around 13:30 LT) and that simulated by the GEOS-CHEM model for northeastern China in August 2006 (Boersma et al., 2008<sup>4</sup>). The ratio derived from MAX-DOAS measurements for June 2006 was  
25  $\sim 1.9$ , which was greater than those from SCIAMACHY/OMI measurements ( $\sim 1.4$ ) and

<sup>4</sup>Boersma, K. F., Jacob, D. J., Eskes, H. J., Pinder, R. W., Wang, J., and van der A, R. J.: Intercomparison of SCIAMACHY and OMI tropospheric NO<sub>2</sub> columns: observing the diurnal evolution of chemistry and emissions from space, submitted to J. Geophys. Res., 2008.

8254

the GEOS-CHEM model ( $\sim 1.3$ ) for August 2006, probably due to the different photochemical loss rate and/or diurnal variation pattern of the  $\text{NO}_x$  emission between the two periods.

### 3.3 Validation of OMI data

5 In Fig. 8a, a time series of the daily mean OMI tropospheric  $\text{NO}_2$  VCDs obtained at locations within  $0.3^\circ$  latitude and longitude of Tai'an is plotted together with MAX-DOAS data. Using this coincident criterion results in 10 coincident MAX-DOAS/OMI pairs (Fig. 8a). The number of coincident pairs was reduced to 4 when a coincident location criterion of  $0.1^\circ$  was used instead (Fig. 8b). For either case the OMI data show  
10 a temporal variation much smaller than that seen in all the MAX-DOAS data (Fig. 6), as the OMI measurements were made only at specific LTs.

For cases with a coincident criterion of  $0.3^\circ$ , we find that the correlations between tropospheric  $\text{NO}_2$  VCDs derived from MAX-DOAS and OMI are rather poor (Fig. 9). This should be partly because the tropospheric  $\text{NO}_2$  VCD at OMI measurement LTs  
15 is invariant over the limited time period analyzed here. The mean difference ( $\pm 1\sigma$  standard deviation) between OMI and MAX-DOAS (OMI minus MAX-DOAS) was estimated to be  $(+2.9 \pm 2.5) \times 10^{15}$  molecules  $\text{cm}^{-2}$  ( $+45 \pm 38\%$ ). In contrast, the use of a stricter coincident location criterion of  $0.1^\circ$  considerably improves the agreement, with the resulting mean difference as small as  $(+1.6 \pm 0.6) \times 10^{15}$  molecules  $\text{cm}^{-2}$  ( $+20 \pm 8\%$ ). This  
20 suggests that such a strict coincident criterion is a prerequisite for accurate validation comparisons.

On the basis of the results for a coincident criterion of  $0.1^\circ$ , it is likely that on average OMI tropospheric  $\text{NO}_2$  data are biased high by  $1.6 \times 10^{15}$  molecules  $\text{cm}^{-2}$  (20%), at least for the locations and the time period of the comparisons made here. A random  
25 error was estimated to be  $0.6 \times 10^{15}$  molecules  $\text{cm}^{-2}$  (8%). Although the number of coincident MAX-DOAS/OMI pairs is small, these estimates are supported by the fact that the comparisons have been made only for 8, 16, 18, and 26 June, when the MAX-DOAS AODs show good agreement with MODIS data (Fig. 3).

8255

Celarier et al. (2008<sup>3</sup>) have summarized results of the validation of OMI tropospheric  $\text{NO}_2$  data for US, Europe, and Pacific Ocean using coincident measurements, including MAX-DOAS measurements during the DANDELIONS (Dutch Aerosol and Nitrogen  
5 Dioxide Experiments for Validation of OMI and SCIAMACHY) (Brinksma et al., 2008<sup>1</sup>) campaign, aircraft measurements during the INTEX (Intercontinental Chemical Transport Experiment)-A, PAVE (Polar Aura Validation Experiment), and INTEX-B campaigns (Bucsela et al., 2008<sup>2</sup>), and the Multi-Function DOAS (MF-DOAS) measurements during the INTEX-B campaign. They investigated the correlations of OMI data with coincident measurement data and concluded that OMI tropospheric  $\text{NO}_2$   
10 column data likely have a negative bias of 15–30%, based on the slope of the linear regression line. It should be noted, however, that some comparisons, especially with MAX-DOAS measurements, revealed that the regression lines have an intercept of  $(3 \pm 1) \times 10^{15}$  molecules  $\text{cm}^{-2}$ , suggesting a positive bias of OMI values. Thus, the bias of OMI data is likely nonconstant over a wide range of tropospheric  $\text{NO}_2$  column  
15 values. In addition, the bias can vary over different regions, for example, through the AMF computation assuming a spatial distribution of the surface albedo. Furthermore, the bias may have a seasonality (Lamsal et al., 2008<sup>5</sup>). Despite these complicated dependencies, however, it is reasonable to conclude here that the OMI tropospheric  $\text{NO}_2$  column data have a bias of  $+20/-30\%$ , which accounts for both our results and the above-mentioned other validation results. To confirm this and diagnose a potential  
20 cause of the bias, a more detailed investigation and more robust comparisons covering a wide range of tropospheric  $\text{NO}_2$  columns and different locations would be necessary.

<sup>5</sup>Lamsal, L. N., Martin, R. V., van Donkelaar, A., Steinbacher, M., Celarier, E. A., Bucsela, E., Dunlea, E. J., and Pinto, J. P.: Ground-level nitrogen dioxide concentrations inferred from the satellite-borne Ozone Monitoring Instrument, submitted to J. Geophys. Res., 2008.

## 4 Conclusions

To validate the OMI tropospheric NO<sub>2</sub> column data (the standard product, version 3) obtained over North China Plain (NCP) for the first time, we performed satellite-independent measurements of the tropospheric NO<sub>2</sub> column using ground-based  
5 MAX-DOAS instruments at two sites (Tai'an and Mt. Tai) in NCP from 29 May to 29 June 2006. For each retrieval of the tropospheric NO<sub>2</sub> column from MAX-DOAS measurements, we used the box-air-mass-factor vertical profiles determined by analyzing the absorption of O<sub>4</sub> with our DOAS method and aerosol retrieval algorithm (Irie et al., 2008). While the AOD values derived from MAX-DOAS O<sub>4</sub> measurements agreed with  
10 MODIS AOD values to within 30% for most cases, MAX-DOAS AOD values tended to be underestimated at MODIS AOD >1.2, due to less sensitivity of the MAX-DOAS measurements to high-altitude aerosols (above ~2 km). However, comparisons between the mean NO<sub>2</sub> VMRs measured by the Tai'an MAX-DOAS for the 1-km layer centered at ~1.6 km with those measured by an in situ instrument at the summit of  
15 Mt. Tai (~1.5 km) showed that the differences were as small as -0.01±0.60 ppbv, supporting the accuracy of MAX-DOAS tropospheric NO<sub>2</sub> data. MAX-DOAS provided the complete diurnal variation of the NO<sub>2</sub> tropospheric VCD (and VMR in the layer for 0 to 1 km) in daytime, with a maximum of ~15×10<sup>15</sup> molecules cm<sup>-2</sup> (~5ppbv) at 06:00–09:00 CST and a minimum of ~7×10<sup>15</sup> molecules cm<sup>-2</sup> (~2 ppbv) at 13:00–15:00 CST,  
20 characterizing the OMI measurements made at the specific LTs around 13:30. Agreement between tropospheric NO<sub>2</sub> columns measured by OMI and MAX-DOAS was improved using a stricter coincident location criterion of 0.1°. The mean difference (±1σ standard deviation) between OMI and MAX-DOAS (OMI minus MAX-DOAS) was then estimated to be (+1.6±0.6)×10<sup>15</sup> molecules cm<sup>-2</sup> (+20±8%). From this result, the random error in OMI data was estimated to be 0.6×10<sup>15</sup> molecules cm<sup>-2</sup> (8%).  
25 Considering other validation results for the US, Europe, and Pacific Ocean (Brinksma et al., 2008<sup>1</sup>; Bucsele et al., 2008<sup>2</sup>; Celarier et al., 2008<sup>3</sup>), the bias was estimated to be +20/–30%, which may depend on the region. These estimates provide the quantitative

8257

basis necessary for analyzing OMI data, especially over NCP.

*Acknowledgements.* The standard product (SP) of OMI NO<sub>2</sub> data was obtained from the NASA Goddard Earth Sciences Data and Information Services Center (GES-DISC). MODIS data were obtained from the NASA LAADS web site. This work was supported by the Global Environment  
5 Research Fund (B-051) of the Ministry of the Environment, Japan. This work was supported by the Ministry of Education, Culture, Sports, Science and Technology (MEXT). This work was supported by Japan EOS (Earth Observation System) Promotion Program of the Ministry of Education, Culture, Sports, Science and Technology (MEXT).

## References

- 10 Boersma, K. F., Eskes, H. J., and Brinksma, E. J.: Error analysis for tropospheric NO<sub>2</sub> retrieval from space, *J. Geophys. Res.*, 109, D04311, doi:10.1029/2003JD003962, 2004.
- Bucsele, E. J., Celarier, E. A., Wenig, M. O., Gleason, J. F., Veefkind, J. P., Boersma, K. F., and Brinksma, E.: Algorithm for NO<sub>2</sub> vertical column retrieval from the Ozone Monitoring Instrument, *IEEE Trans. Geosci. Remote Sens.*, 44(5), 1–14, 2006.
- 15 Frieß, U., Monks, P. S., Remedios, J. J., Rozanov, A., Sinreich, R., Wagner, T., and Platt, U.: MAX-DOAS O<sub>4</sub> measurements: A new technique to derive information on atmospheric aerosols: 2. Modeling studies, *J. Geophys. Res.*, 111, D14203, doi:10.1029/2005JD006618, 2006.
- Fu, T.-M., Jacob, D. J., Palmer, P. I., Chance, K., Wang, Y. X., Barletta, B., Blake, D. R., Stanton, J. C., and Pilling, M. J.: Space-based formaldehyde measurements as constraints on volatile organic compound emissions in east and south Asia and implications for ozone, *J. Geophys. Res.*, 112, D06312, doi:10.1029/2006JD007853, 2007.
- Hönninger, G., von Friedeburg, C., and Platt, U.: Multi axis differential optical absorption spectroscopy (MAX-DOAS), *Atmos. Chem. Phys.*, 4, 231–254, 2004,  
25 <http://www.atmos-chem-phys.net/4/231/2004/>.
- Inomata, S., Tanimoto, H., Kameyama, S., Tsunogai, U., Irie, H., Kanaya, Y., and Wang, Z.: Technical note: Determination of formaldehyde mixing ratios in air with PTR-MS: Laboratory experiments and field measurements, *Atmos. Chem. Phys.*, 8, 273–284, 2008, <http://www.atmos-chem-phys.net/8/273/2008/>.

8258

- Irie, H., Sudo, K., Akimoto, H., Richter, A., Burrows, J. P., Wagner, T., Wenig, M., Beirle, S., Kondo, Y., Sinyakov, V. P., and Goutail, F.: Evaluation of long-term tropospheric NO<sub>2</sub> data obtained by GOME over East Asia in 1996–2002, *Geophys. Res. Lett.*, 32, L11810, doi:10.1029/2005GL022770, 2005.
- 5 Irie, H., Kanaya, Y., Akimoto, H., Iwabuchi, H., Shimizu, A., and Aoki, K.: Performance of MAX-DOAS measurements of aerosols at Tsukuba, Japan: a comparison with lidar and sky radiometer measurements, *Atmos. Chem. Phys.*, 8, 341–350, 2008, <http://www.atmos-chem-phys.net/8/341/2008/>.
- Iwabuchi, H.: Efficient Monte Carlo methods for radiative transfer modeling, *J. Atmos. Sci.*, 63, 9, 2324–2339, 2006.
- 10 Jacobson, M. Z.: *Fundamentals of atmospheric modeling*, Cambridge University Press, 1999.
- Levelt, P. F., van den Oord, G. H. J., Dobber, M. R., Mälkki, A., Visser, H., de Vries, J., Stammes, P., Lundell, J. O. V., and Saari, H.: The Ozone Monitoring Instrument, *IEEE Trans. Geosci. Remote Sens.*, 44, 5, 1093–1101, 2006.
- 15 Remer, L. A., Kaufman, Y. J., Tanré, D., Mattoo, S., Chu, D. A., Martins, J. V., Li, R.-R., Ichoku, C., Levy, R. C., Kleidman, R. G., Eck, T. F., Vermote, E., and Holben, B. N.: The MODIS aerosol algorithm, products, and validation, *J. Atmos. Sci.*, 62, 4, 947–973, doi:10.1175/JAS3385.1, 2005.
- Richter, A., Burrows, J. P., Nüß, H., Granier, C., and Niemeier, U.: Increase in tropospheric nitrogen dioxide over China observed from space, *Nature*, 437, 129–132, doi:10.1038/nature04092, 2005.
- 20 Rodgers, C. D.: *Inverse methods for atmospheric sounding: Theory and practice*, Ser. Atmos. Oceanic Planet. Phys., 2, edited by: F.W. Taylor, World Sci., Hackensack, N.J., 2000.
- van der A, R. J., Peters, D. H. M. U., Eskes, H., Boersma, K. F., van Roozendaal, M., de Smedt, I., and Kelder, H. M.: Detection of the trend and seasonal variation in tropospheric NO<sub>2</sub> over China, 111, D12317, doi:10.1029/2005JD006594, 2006.
- van Noije, T. P. C., Eskes, H. J., Dentener, F. J., Stevenson, D. S., Ellingsen, K., Schultz, M. G., Wild, O., Amann, M., Atherton, C. S., Bergmann, D. J., Bey, I., Boersma, K. F., Butler, T., Cofala, J., Drevet, J., Fiore, A. M., Gauss, M., Hauglustaine, D. A., Horowitz, L. W., Isaksen, I. S. A., Krol, M. C., Lamarque, J.-F., Lawrence, M. G., Martin, R. V., Montanaro, V., Müller, J.-F., Pitari, G., Prather, M. J., Pyle, J. A., Richter, A., Rodriguez, J. M., Savage, N. H., Strahan, S. E., Sudo, K., Szopa, S., and van Roozendaal, M.: Multi-model ensemble simulations of tropospheric NO<sub>2</sub> compared with GOME retrievals for the year 2000, *Atmos. Chem. Phys.*,

8259

- 6, 2943–2979, 2006, <http://www.atmos-chem-phys.net/6/2943/2006/>.
- Wagner, T., Burrows, J. P., Deutschmann, T., Dix, B., von Friedeburg, C., Frieß, U., Hendrick, F., Heue, K.-P., Irie, H., Iwabuchi, H., Kanaya, Y., Keller, J., McLinden, C. A., Oetjen, H., 5 Palazzi, E., Petritoli, A., Platt, U., Postlyakov, O., Pukite, J., Richter, A., van Roozendaal, M., Rozanov, A., Rozanov, V., Sinreich, R., Sanghavi, S., and Wittrock, F.: Comparison of box-air-mass-factors and radiances for multiple-axis differential optical absorption spectroscopy (MAX-DOAS) geometries calculated from different UV/visible radiative transfer models, *Atmos. Chem. Phys.*, 7, 1809–1833, 2007, <http://www.atmos-chem-phys.net/7/1809/2007/>.
- 10

**Table 1.** Median values of the absolute and relative errors ( $\pm(\text{systematic error})\pm(1\sigma \text{ random error})$ ), the maximum box-air-mass-factors ( $A_{\text{box,max}}$ ), and the horizontal distances ( $D$ ) for MAX-DOAS  $\text{NO}_2$  measurements at Tai'an.

	Abs. err. <sup>a</sup>	Rel. err. (%)	$A_{\text{box,max}}$	$D(\text{km})$
VCD	$\pm 1.0\pm 0.5$	$\pm 11\pm 5$	–	–
VMR 0–1 km	$\pm 0.3\pm 0.3$	$\pm 9\pm 11$	3.8	3.7
VMR 1–2 km	$\pm 0.1\pm 0.2$	$\pm 8\pm 28$	2.7	2.5

<sup>a</sup> Units are  $10^{15}$  molecules  $\text{cm}^{-2}$  and ppbv for VCD and VMR, respectively.

8261

**Table 2.** Same as Table 1, but for MAX-DOAS measurements at Mt. Tai.

	Abs. err. <sup>a</sup>	Rel. err. (%)	$A_{\text{box,max}}$	$D(\text{km})$
VCD	$(\pm 0.6\pm 1.1)^{\text{b}}$	$(\pm 7\pm 12)^{\text{a}}$	–	–
VMR 0–1 km	$(\pm 0.2\pm 0.6)^{\text{b}}$	$(\pm 6\pm 19)^{\text{a}}$	1.2	0.7
VMR 1–2 km	$\pm 0.1\pm 0.3$	$\pm 10\pm 47$	5.1	5.0

<sup>a</sup> Units are  $10^{15}$  molecules  $\text{cm}^{-2}$  and ppbv for VCD and VMR, respectively.

<sup>b</sup> Note that the errors can be greater due to the insufficient penetration of the measured sunlight for the 0–1-km layer, as discussed in the text.

8262

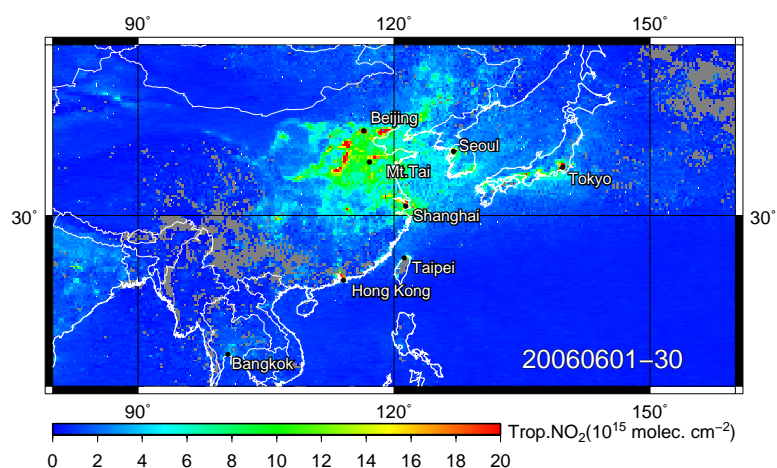


**Fig. 1.** Monthly mean tropospheric NO<sub>2</sub> columns measured by OMI in June 2006. Data with a cloud fraction less than 0.1 were plotted on a 0.25° (in latitude) × 0.25° (in longitude) grid. Values exceeding 20 × 10<sup>15</sup> molecules cm<sup>-2</sup> are shown in red. MAX-DOAS measurements were made at and near the location indicated by “Mt. Tai.” Tai’an was located only 10 km south of Mt. Tai.

8263

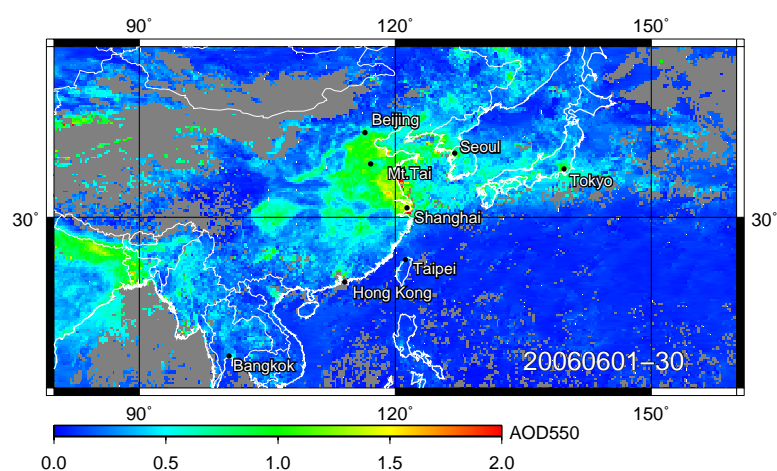


**Fig. 2.** Same as Fig. 1, but for AOD at 550 nm measured by MODIS instruments. The MODIS data with a cloud fraction less than 0.1 were used. Two datasets, from MODIS/Terra and MODIS/Aqua, have been unified.

8264

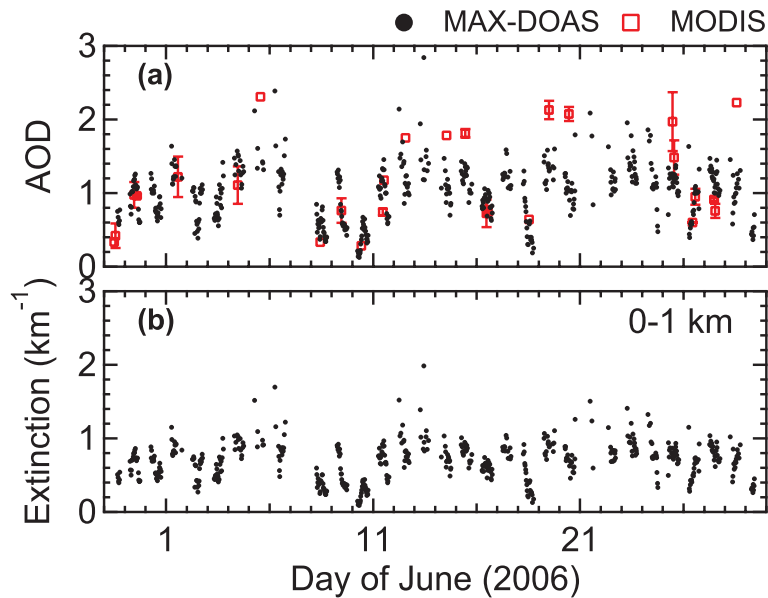


**Fig. 3.** (a) Time series of AOD values at 476 nm derived from MAX-DOAS measurements at Tai'an (black). Mean AOD values obtained by MODIS within 0.1° latitude and longitude of Tai'an are also shown in red. Error bars represent 1 $\sigma$  standard deviations. Two MODIS datasets from Terra and Aqua satellites have been averaged separately but are plotted with the same symbols for simplicity. The MODIS data with a cloud fraction less than 0.1 were used. The original MODIS AOD values at 470 nm have been converted to the values at 476 nm using the Ångström exponent. (b) Time series of MAX-DOAS-derived AEC values for the lowest 1-km layer above the surface is shown.

8265

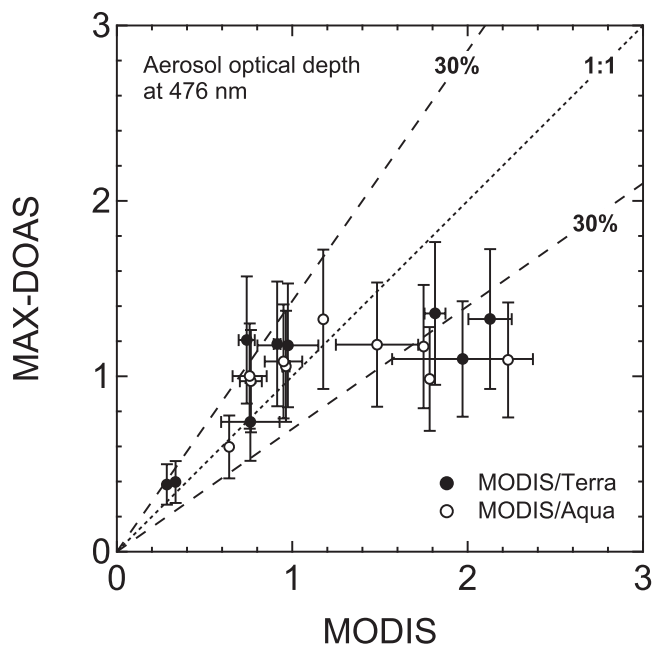


**Fig. 4.** Correlations between AOD values at 476 nm derived from MAX-DOAS and MODIS. Two MODIS datasets from Terra and Aqua are shown with solid and open symbols, respectively. The 1:1 relationship and the 30% range are represented by the dotted line and dashed lines, respectively.

8266

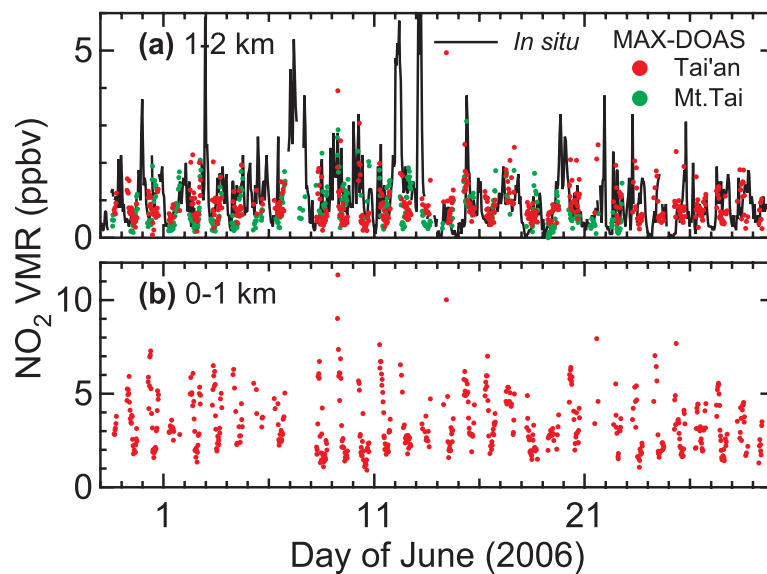


**Fig. 5.** (a) Time series of the mean  $\text{NO}_2$  volume mixing ratios (VMRs) for the 1–2-km layer above the surface ( $\sim 1.6 \pm 0.5$  km a.s.l.) derived from MAX-DOAS measurements at Tai'an (red) and Mt. Tai (green). In situ  $\text{NO}_2$  data obtained at the top of Mt. Tai ( $\sim 1.5$  km a.s.l.) are also shown in black. (b) Time series of the mean  $\text{NO}_2$  VMRs derived from MAX-DOAS measurements at Tai'an is shown for the 0–1-km layer above the surface.

8267

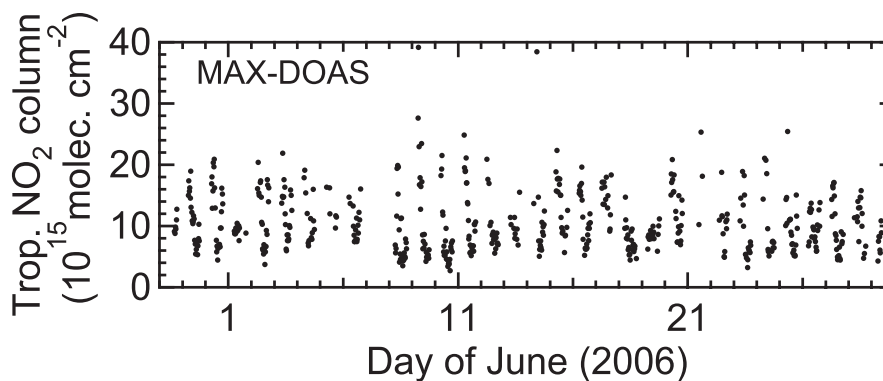


**Fig. 6.** Time series of all the MAX-DOAS data of tropospheric  $\text{NO}_2$  columns at Tai'an.

8268

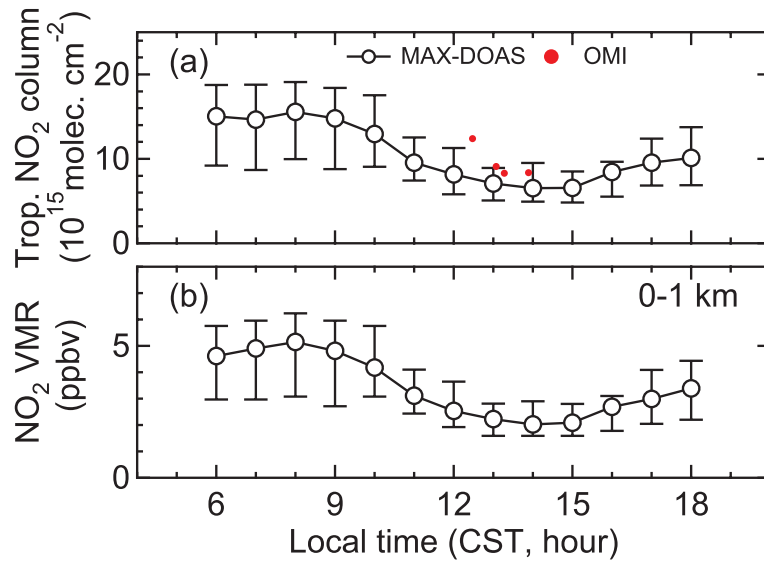


**Fig. 7.** (a) Median diurnal variation of the tropospheric NO<sub>2</sub> columns measured by MAX-DOAS at Tai'an over the period from 29 May to 29 June 2006. Error bars represent 67% ranges. Daily mean OMI data obtained within 0.1° latitude and longitude of Tai'an are also plotted in red. The local time is the Chinese standard time. (b) Same as (a), but for the mean MAX-DOAS NO<sub>2</sub> VMR values for the 0–1-km layer above the surface.

8269

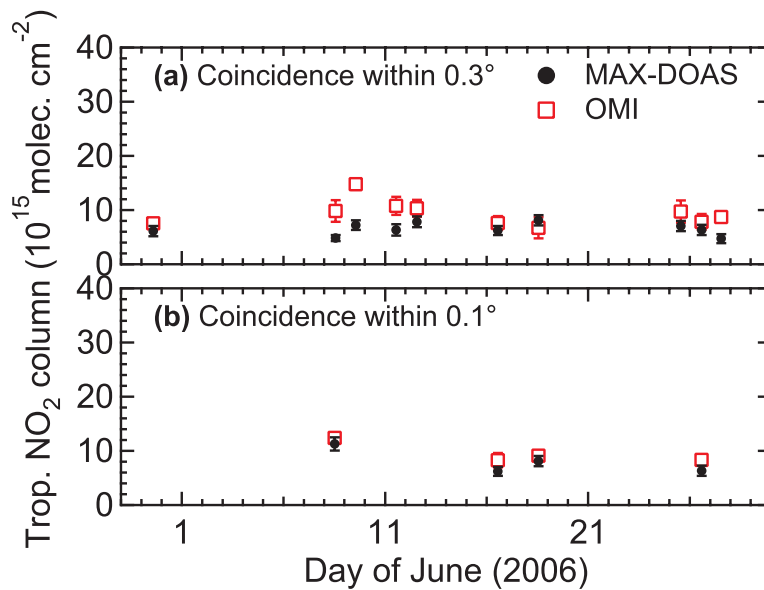


**Fig. 8.** Coincident pairs of Tai'an MAX-DOAS (black) and OMI (red) selected with coincident location criteria of (a) 0.3° and (b) 0.1°. Daily mean OMI data over Tai'an are plotted. Error bars represent 1σ standard deviations.

8270

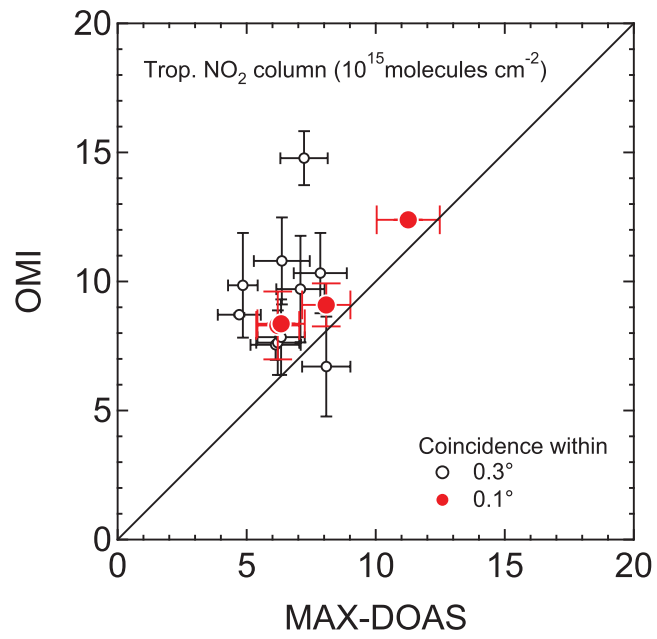


**Fig. 9.** Correlations between tropospheric NO<sub>2</sub> columns derived from MAX-DOAS and OMI. The pairs selected by the different coincident criteria of 0.3° and 0.1° are shown in black and red, respectively.